Impact of Dissociation Constant on the Detection Sensitivity of Polymerization-Based Signal Amplification Reactions

Citation: Kaastrup, Kaja, Leslie Chan, and Hadley D. Sikes. "Impact of Dissociation Constant on the Detection Sensitivity of Polymerization-Based Signal Amplification Reactions." Analytical Chemistry 85, no. 17 (September 3, 2013): 8055–8060.

As Published: http://dx.doi.org/10.1021/ac4018988

Publisher: American Chemical Society (ACS)

Persistent URL: http://hdl.handle.net/1721.1/94340

Version: Author's final manuscript: final author's manuscript post peer review, without publisher's formatting or copy editing

The impact of dissociation constant on the detection sensitivity of polymerization-based signal amplification reactions

Kaja Kaastrup, Leslie Chan, and Hadley D. Sikes*

Department of Chemical Engineering, Massachusetts Institute of Technology, Cambridge, MA 02139

* To whom correspondence should be addressed
Tel: 617-324-4870
Fax: 617-253-2272
Email: sikes@mit.edu

Abstract

Many studies have demonstrated the concept of using free-radical polymerization reactions to provide signal amplification so that molecular recognition events indicative of disease states may be detected in a simple and low-cost manner. We provide the first systematic study of how dissociation constant impacts detection sensitivity in these assays, having chosen a range of dissociation constants (nanomolar to picomolar) that is typical of those encountered in molecular diagnostic applications that detect protein-protein binding events. In addition, we use experimental results to validate a mass-action kinetic model that may be used to predict assay performance as an alternative or supplement to the empirical approach to developing new polymerization-based amplification assays that has characterized the field to date.

Introduction

Polymerization-based amplification has been established as a sensitive signal amplification technique for use in molecular diagnostics.[1–22] Amplification is achieved through the initiation of radical polymerization coupled to molecular recognition at a surface. Initiating molecules immobilized at a surface generate radical species that react with carbon-carbon double bonds of acrylate monomers, a process that results in polymer formation. Various chemistries have been implemented, including atom transfer radical polymerization (ATRP),[1,11,12,23,24] photopolymerization,[2,4–9,13,15–17,20,22] reversible addition-fragmentation chain transfer polymerization (RAFT),[3,10,19] and enzyme-mediated redox polymerization.[18,21] Of these methods, photopolymerization has shown promise as a point-of-care technology as it allows for the formation of micron scale hydrogels in as little as thirty-five seconds under ambient conditions.[22]

Photopolymerization-based amplification requires the localization of photoinitiators at a surface through binding events (typically DNA hybridization or protein binding). Much of the previous work studying photopolymerization-based amplification has explored the case in which signal amplification, rather than the thermodynamics or kinetics of the binding event, is limiting.[2,4–7,9,15,18,20–22] These studies have made use of the high-affinity biotin-avidin interaction (dissociation constant~10^{-15} M)[25] as a model recognition event that is particularly well suited to studying the effects of varying different aspects of the chemistry, such as monomer composition or initiator type. However, in order to implement this technology for clinical diagnostics, it is necessary to employ biological recognition events for which dissociation constants (K_d) are typically in the nanomolar to picomolar range (e.g. antibody-antigen complex formation).[26]

Although there are several examples of polymerization-based amplification studies involving antibody-antigen complex formation,[7,12–15,17,18,21,23] a systematic investigation of the effect of varying the dissociation constant on assay sensitivity has never been performed. In the absence of signal amplification, it is expected that increasing the binding affinity should enhance the sensitivity of an assay. However, the coupling of a binding event with an amplification reaction introduces additional complexities. For amplification processes, there are generally three distinct signal regimes. The first regime, near the limit of detection, is set by the amplification threshold. In the case of photopolymerization, this threshold corresponds to the minimum initiator density required to induce polymerization. For enzyme-linked immunosorbent assay (ELISA), the threshold is set by the minimum amount of enzyme necessary for sufficient substrate conversion for a detectable readout, and for immuno-PCR, the threshold is the minimum DNA concentration required for PCR. The second signal regime is characterized by dynamic change in the signal in response to initiator, enzyme, or DNA concentration changes, and in the final regime, above a certain initiator, enzyme, or DNA surface concentration, amplification based assays tend to exhibit signal plateaus.[6,27] In this final regime, there may be no apparent difference between binding molecules with different dissociation constants depending on the concentration used and whether that concentration results in a fraction bound that is within the plateau region. For the purposes of bioassay development, quantitatively establishing how these signal regimes relate to K_d values is useful, particularly in the nanomolar to picomolar range.

Binding affinity studies of ELISAs have predominantly shown that assay sensitivity improves as the dissociation constant for the interaction decreases.[28,29] However, in a study by Glass et al. in which the least detectable concentration (LDC) was measured for four antibodies for estradiol

with different affinities (K_d=0.006 to 1.4 nM as measured by kinetic exclusion), the authors measured the same LDC for the two highest affinity binders.[29] In the absence of experimental details such as the length of the incubation periods (data collection was contracted out to the biosensor manufacturer), it is difficult to speculate as to why the LDC did not change when the K_d was reduced from 0.039 to 0.006 nM.

In this study, we investigate the impact of varying binding affinity on the sensitivity of photopolymerization-based amplification using three fibronectin clones that have been engineered to bind to the epidermal growth factor receptor (EGFR) ectodomain with different affinities (K_d=250 pM-30 nM).[30] The proteins are engineered such that mutations of a small subset of amino acids alter binding affinity without dramatically changing other properties of the protein; this allows for an evaluation based on binding affinity without the introduction of additional variables. Keeping other parameters constant, the concentration of each of the clones was reduced until polymerization was no longer observed. We then tested the applicability of a mass-action kinetic model of protein binding for predicting the minimum surface initiator density required for polymerization.

Experimental

Protein Preparation and Characterization

The affinities of fibronectin clones B, D, and E for EGFR were previously determined by titration of the biotinylated clones to A431 cells.[30] Plasmids (pEThK-Fn3 clones B, D, and E)[30] obtained from the K. D. Wittrup Lab were transformed into Rosetta (DE3) E. coli and grown in LB medium (with 30 mg/L kanamycin and 25 mg/L chloramphenicol) at 37°C. Following

expression (induced with IPTG), the cells were lysed and pelleted. The supernatant was sterile filtered and the proteins were purified using metal-affinity chromatography (Supplementary Figure 1).

Following purification, the proteins were biotinylated with EZ-Link NHS-LC-Biotin and subsequently purified using UltraCruz™ Micro G-25 Spin Columns. Total protein was quantified using a BCA assay with BSA standards. The degree of biotinylation was determined using a HABA (4'-hydroxyazobenzene-2-carboxylic acid) assay (Supplementary Figure 2). The fraction of the total protein corresponding to each of the fibronectin clones was estimated using densitometry (Supplementary Figure 3).

Preparation of Detection Reagents

A macrophotoinitiator capable of binding biotin was prepared by coupling eosin initiators to streptavidin by reaction of eosin 5-isothiocyanate with a fraction of the solvent-accessible lysine residues of streptavidin as previously described.[4] The aqueous monomer solution consisted of 0.5 μM eosin, 200 mM poly(ethylene glycol) diacrylate (PEGDA) (M_n=575), 100 mM triethanolamine (TEA), and 150 mM 1-vinyl-2-pyrrolidinone (VP).

Test surface preparation

Aldehyde functionalized agarose surfaces were prepared according to published methods.[31] Each test surface consisted of duplicate spots of 0.1 μL 250 μg/mL EGFR (Supplementary Figure 4) in PBS, one spot of BSA (0.1 μL 250 μg/mL in PBS) as a negative control, and one spot of biotinylated fibronectin clone B (0.1 μL 250 μg/mL in PBS) as a positive control for

macrophotoinitator binding and polymerization. Post-spotting, the surfaces were kept at ambient conditions overnight. Silicone isolator wells were applied in order to confine the monomer to the test area during polymerization. The number of binding-accessible EGFR molecules per square micron in each spot was quantified using a streptavidin-Cy3 conjugate and fluorescence analysis.

Detection of molecular recognition using PBA

To reduce the incidence of nonspecific binding, the test surfaces were first blocked with 1% BSA in 1x PBS for 10 minutes. Following a rinse with PBS, the surfaces were contacted with one of the three biotinylated fibronectin clones at total protein concentrations ranging between 0.1 and 10 μg/mL. The total protein concentration (as measured with a BCA assay) was kept constant, rather than the concentrations of the individual clones, in recognition of the fact that any contaminant proteins present would have also been functionalized with biotin. Keeping total protein concentration constant ensured that levels of non-specific binding would be held constant. To begin an assay, 40 μL of one of the biotinylated fibronectin clones (0.1-10 μg/mL with 1% BSA in 1x PBS) was added to each of the isolators wells. After 30 minutes (at which point it was assumed that binding was complete), the surfaces were rinsed once more with 1x PBS and contacted with 40 μL of 0.1 μM (6 μg/mL streptavidin) streptavidin-eosin in 0.75% BSA, 1.5x PBS and 5x Denhardt's Solution for 5 minutes in a humid chamber. To remove unbound initiator, surfaces were rinsed with PBST (1x PBS, 0.1% Tween 20), 1x PBS, and distilled water and wicked dry. Once dry, 40 μL of the prepared monomer solution was contacted with the surface and the surface was irradiated with 522 nm light (30 mW/cm^2, measured using a SPER Scientific Light Meter) from an array of LEDs housed in an ampliPHOX® reader (InDevR) for 100 seconds. Unreacted monomer solution was removed by rinsing the surface

with distilled water. Remaining hydrogel surface features, if present, were stained with 50 mM eosin (50% methanol, 50% distilled water) for 2 minutes and subsequently rinsed with water to allow visualization of the polymer on the slide surface. Each condition was repeated a minimum of 5 times. Two control experiments were performed to verify the specificity of the interaction between surface immobilized biotin and the macrophotoinitiator as well as that between EGFR and the three fibronectin clones. In the first experiment, 10 μg/mL of each of the *unbiotinylated* fibronectin clones was used in place of their biotinylated counterparts. In the second experiment, the test surface development was performed omitting the fibronectin binding step so that the surfaces were only contacted with streptavidin-eosin. These experiments were performed to assess the specificity of the polymerization response; assay conditions must be chosen such that streptavidin-eosin does not nonspecifically bind EGFR or the fibronectin clones at a level sufficient for the initiation of polymerization.

Analysis

Each surface was imaged using the digital camera built into the ampliPHOX® Reader (InDevR) imaging bay. Mean intensity and standard deviation values were calculated for every surface feature and for the background in an automated fashion using the ampliVIEW® software that accompanies the instrument.

Full details of the chemical suppliers and experimental methods are provided in the supplementary information.

Results and Discussion

A schematic of the binding events resulting in polymerization is presented in Figure 1. As depicted, biotinylated fibronectin binds to EGFR immobilized on activated agarose (K_d=0.25-30 nM depending on the clone), and this is followed by the binding reaction between biotin and the streptavidin of the macrophotoinitiator. Streptavidin is coupled to a photoinitiator, eosin, which, in the presence of a co-initiator (triethanolamine), can induce radical polymerization in response to light in the visible range (522 nm). The resulting hydrogel is stained with a dye for ease of visualization; the final result is depicted in Figure 2 for fibronectin clone D. For the radical polymerization reaction, eosin is present both at the surface as a function of the sequential binding events as well as in the bulk monomer solution in order to circumvent the oxygen inhibition typical of radical photopolymerization reactions.[22] The polymerization is a threshold process, and thus will be limited to the surface where the local concentration of eosin is higher than in the bulk solution provided that local concentration exceeds a minimum initiator threshold. Thresholds are also encountered in ELISA and immuno-PCR[27] for which signal plateaus are observed above a certain enzyme or DNA concentration.

Figure 2 shows that polymerization is restricted to those areas in which eosin has been immobilized as function of the two binding events. There is no polymerization on the surface where BSA has been immobilized; BSA should have little affinity for the EGFR binders and streptavidin-eosin. The positive control spot consisting of biotinylated protein serves to validate the activity of the macrophotoinitiator as well as of the monomer solution. To ensure that polymerization is obtained only in response to the two sequential binding interactions, two control experiments were performed (Supplementary Figure 5). In the first, unbiotinylated fibronectin clones were used in place of the biotinylated clones to confirm that the macrophotoinitiator binding is a result of the interaction between biotin and streptavidin. In order

to exclude the possibility of polymerization resulting from nonspecific binding of streptavidin-eosin to EGFR, a second control experiment was performed in which the fibronectin was excluded.

The colorimetric intensity of the stained hydrogels was averaged (5 trials) for the EGFR binders at each of the concentrations assayed (Figure 3). The correlation between binder affinity and the concentration required to achieve sufficient surface coverage to initiate polymerization is apparent. Polymerization was observed for concentrations of the highest affinity binder (clone D, K_d=0.25 nM) at a concentration as low as 6 nM. For both clones E (K_d=2.9 nM) and B (K_d=30 nM), no polymerization was observed below 10 nM. However, sufficient binding for polymerization was achieved for surfaces contacted with 20 nM clone E. It is noteworthy that both clone D and clone B performed inconsistently at their respective concentration limits (6 nM and 47 nM), initiating polymerization in 3 of 5 trials. This suggests that the complex concentration (number of biotinylated fibronectins bound) on the surface approaches the initiator threshold that must be exceeded for polymerization at these concentrations and the amount of active EGFR immobilized on the surface is limiting.

Near the limit of detection, small differences in the number of protein molecules bound (or immobilized on the surface) dictate whether or not the threshold for polymerization is exceeded. The threshold nature of the polymeric amplification[2,16] is also seen in the lack of correlation between the extent of the polymerization (as indicated by the colorimetric intensity[20]) and the binder concentration used, although it is likely that the fractional surface coverage increases with binder concentration. Further indication that a threshold limit based on the number of surface-

immobilized protein molecules has been reached, the concentration limit for clone B is approximately 1.5 times its dissociation constant, while the concentration limit for clone D is more than an order of magnitude greater than its dissociation constant. This suggests that increasing the concentration of active surface immobilized EGFR would allow for further reductions in the fibronectin clone concentrations necessary for achieving a surface initiator density sufficient for polymerization. Johnson et al. demonstrated the effects of altering the relative concentrations of the capture and probe molecules for a nucleic acid hybridization study.[16] Near the limit of detection (78 capture DNA/ μm^2), they found that a concentration of 10 nM target DNA is necessary for the formation of a polymer film, while increasing the capture density to 6500/ μm^2 allows for a reduction in the target DNA concentration to below 0.5 nM.[16] Similarly, simulation shows that as the EGFR surface density is increased, the fraction of available binding sites occupied remains the same, but the overall number of fibronectin clones bound per unit area increases (Supplementary Figure 6).

In order to determine the surface initiator density threshold for polymerization, it is useful to calculate the theoretical fraction of EGFR molecules bound for each of the clones at the concentrations assayed. The reversible bimolecular interaction at the surface can be written as $L + P$ Ä C where L represents the binding ligand, P the surface-immobilized protein, and C the complex formed at the surface. Assuming mass action kinetics, the rate of association takes the form $k_{on}[L][P]$ and the dissociation rate takes the form $k_{off}[C]$ (where brackets are used to indicate concentration and k_{on} and k_{off} are kinetic constants with units of $M^{-1}s^{-1}$ and s^{-1}, respectively). The rate of change of complex can be expressed as follows:

$$\frac{dC}{dt} = k_{on}[L][P] - k_{off}[C]$$

Provided that the ligand is present in excess of the protein immobilized on the surface and the rate of ligand diffusion to the surface is faster than the rate of association, the ligand concentration can be taken as constant. An analysis of the Damkohler number, which is defined as the ratio of the reaction velocity $k_{on}[L]$ to the diffusion velocity D/h (where k_{on} is the on-rate for ligand binding, [L] is the concentration of ligand a distance h away from the surface, and D is the diffusivity of the ligand through the medium) supports this simplification. An approximation for the Damkohler number over the depth of the liquid was obtained by calculating the ligand diffusivity according to the Stokes-Einstein equation (Figure 4). Over the range of ligand concentrations and depths assayed, the Damkohler number is much less than 1, indicating that the rate of diffusion to the surface is significantly faster than the reaction at the surface; binding is reaction-limited and the ligand concentration at the surface is essentially constant.

Assuming ligand excess and a typical order-of-magnitude value of 10^5 $M^{-1}s^{-1}$ for k_{on} [32] and using the dissociation constant to determine k_{off} ($K_d = \frac{k_{off}}{k_{on}}$), a plot showing the complex concentration after a 30-minute incubation period as a function of fibronectin clone concentration for each of the three binders was generated (Figure 5). Comparing the experimental results with the complex concentrations output by this model indicates that the threshold for polymerization is 140 protein molecules/μm^2. The EGFR density on the surface was set at 230 molecules/μm^2 based on fluorescent labeling and comparison with a calibration array (Supplementary Figure 7). This

model shows that the theoretical complex concentration for surfaces contacted with 10 nM clone E is greater than that for 6 nM clone D, although polymerization was only observed in the case of the latter. This discrepancy could be explained by the assumption of an on-rate of 10^5 $M^{-1}s^{-1}$ for all clones. These clones were selected using equilibrium screening and the on-rates were never directly determined,[30] so it is possible that the on-rates could differ slightly for any of the three clones. A reduced on-rate for clone E would result in a lower surface complex concentration (Supplementary Figure 8). Assuming an on-rate of 10^5 $M^{-1}s^{-1}$, the model predicts a complex concentration of 160 molecules/μm^2, which is above the threshold for polymerization. However, fluorescence-based surface density quantification (Supplementary Figure 9) reveals that only 70 molecules/μm^2 are bound, a result consistent with a lower on-rate and the absence of polymerization.

Conclusions

In the study of the impact of dissociation constant on the observed detection sensitivity using polymerization-based signal amplification reactions presented here, our key findings are that within the parameter space investigated, improvements in binding affinity lead to marked improvements in detection sensitivity. Experimental findings were accurately predicted using a mass action kinetic model. Combined model and experimental findings support the idea that in polymerization-based amplification assays, detection sensitivity for a solution phase molecule is determined by whether a threshold initiator surface density is attained as a result of the kinetic and thermodynamic characteristics of the chosen recognition events and the chosen assay conditions (incubation time, surface capture probe density). Bioassay development is typically an empirical process that can be time consuming and costly. The ability to predict assay

performance greatly enhances the efficiency of this process. As presented here, a simple kinetic model can be used to predict assay performance given a minimal set of experimentally accessible parameters (surface capture probe density and binding affinity).

In addition, experimental validation of this simple model in the context of polymerization-based amplification assays is valuable for future efforts to engineer binding reagents since improved assay performance as a function of improvements in binding affinity may be quantitatively predicted prior to committing resources to a protein engineering effort. This work also provides guidance in assessing whether commercial binding reagents are likely to provide adequate sensitivity in a given application.

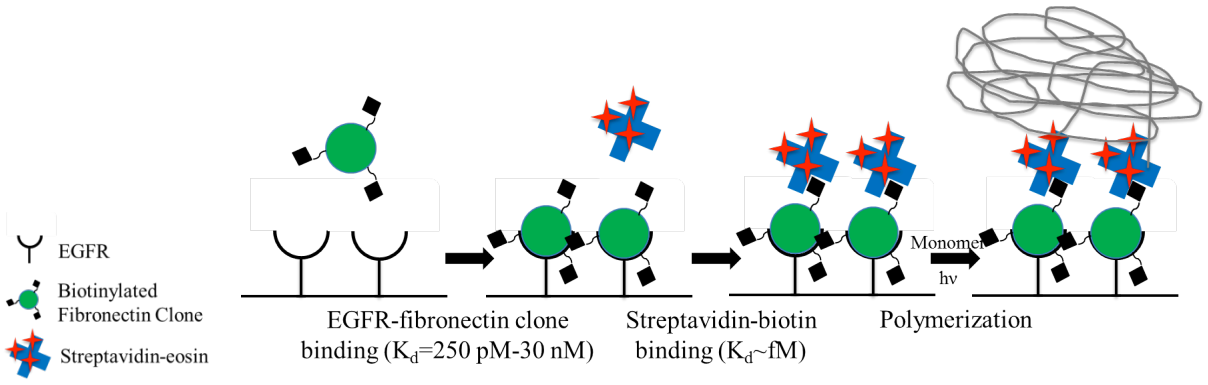

Figure 1. Schematic of the binding interactions that lead to polymerization. Biotinylated fibronectin clones engineered to bind with varying affinities to EGFR are bound by the surface-immobilized EGFR. A photoinitiator, eosin, is then tethered at the surface through the binding of a streptavidin-eosin conjugate to biotin. With the addition of a monomer solution containing a co-initiator (triethanolamine), eosin then induces radical polymerization in response to light in the visible range (522 nm). This results in a hydrogel confined to regions where initiating molecules have been immobilized.

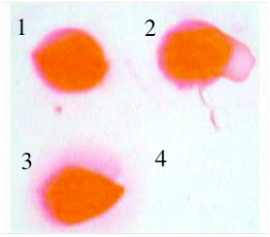

Feature	Mean	Standard Deviation	Recognition Event	Function
1	135.1	3.5	EGFR : Fn3-b : SA	Test site
2	130.4	7.2	EGFR : Fn3-b : SA	Test site
3	131.7	3.7	Fn-b : SA	Positive control
4	23.4	1.1	BSA	Negative control

Figure 2. Colorimetric detection of clone D binding to surface immobilized EGFR. The concentration of clone D in solution was 1 uM. Features 1 and 2 are stained hydrogels generated in response to two subsequent binding events. First, biotinylated clone D binds to surface immobilized EGFR. This is followed by the binding of streptavidin-eosin. Feature 3 is a positive control for the polymerization reaction. In this case, streptavidin-eosin binds to biotinylated protein immobilized on the surface. Feature 4 is a negative control consisting of surface immobilized BSA. The mean and standard deviation values reported in the accompanying table derive from the quantification of the pixel intensities comprising each feature in the digital image and are based on areas incorporating the majority of each feature, but excluding edge effects.

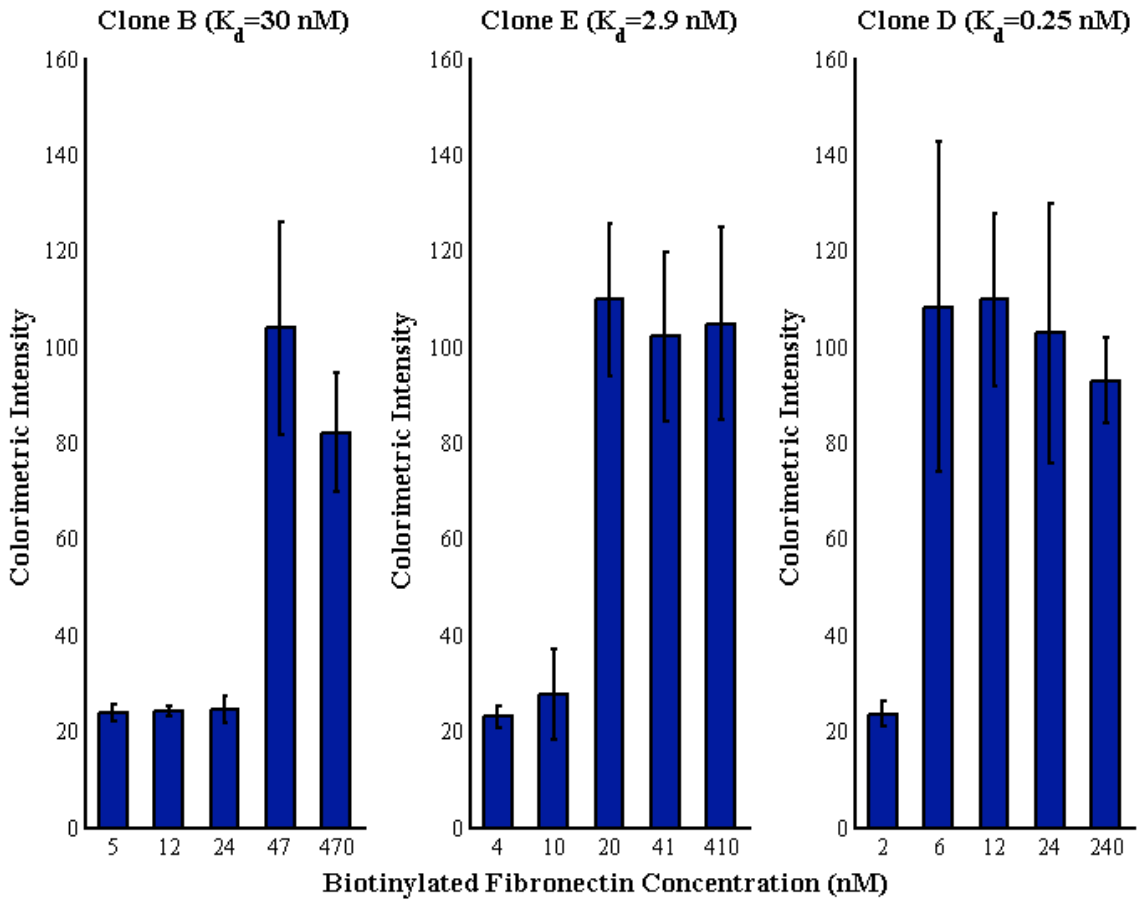

Figure 3. Colorimetric intensity of the polymerization response for each of the fibronectin clones as a function of concentration. The concentrations are calculated from the total protein concentration based on SDS-PAGE gel densitometry. In the case of clone D at a concentration of 6 nM, a positive response was obtained in 3 of 5 trials. Similarly, for 47 nM clone B, a positive response was obtained in 3 of 5 trials. The colorimetric intensity of the agarose surface (the background) was ~25.

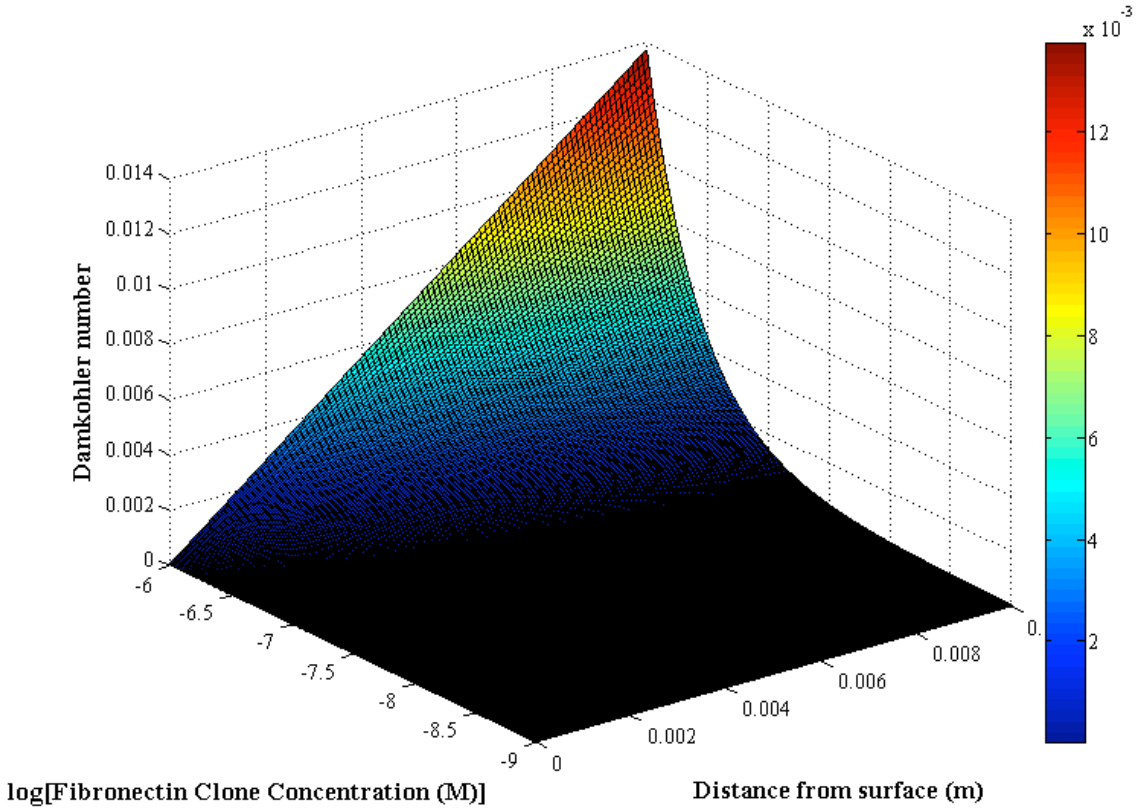

Figure 4. Damkohler number as a function of both fibronectin clone concentration and the distance between the fibronectin clone in solution and the EGFR on the surface.

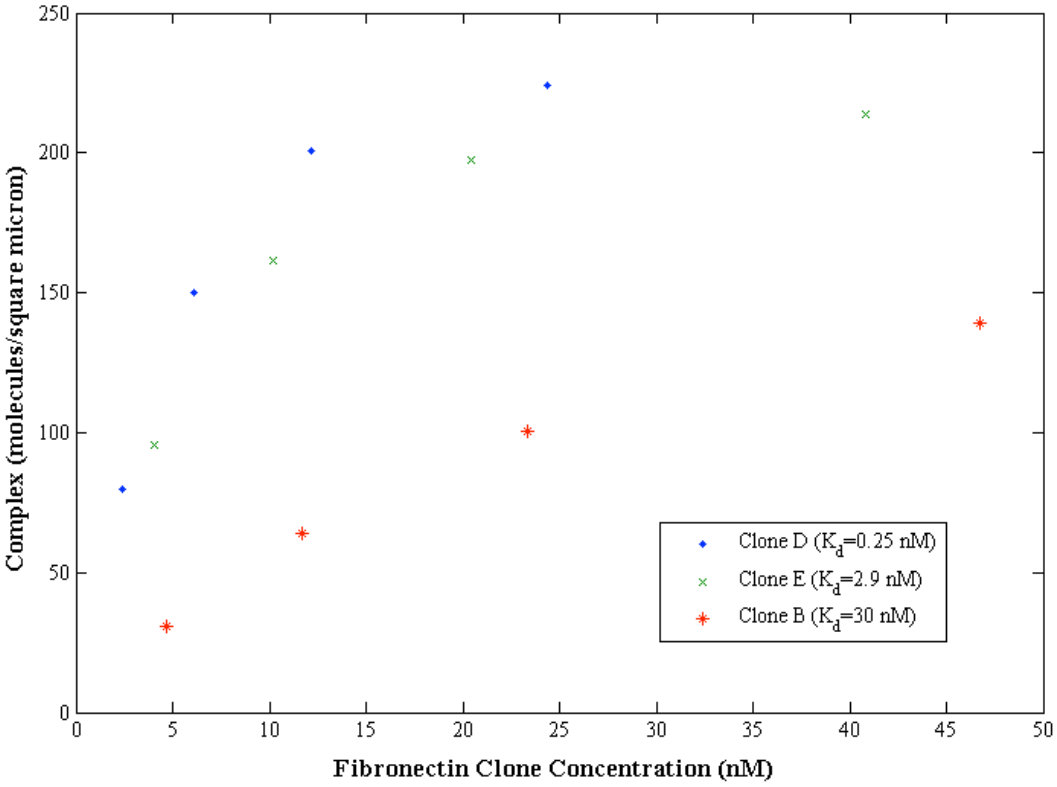

Figure 5. Theoretical surface concentrations of the EGFR-fibronectin complex as a function of solution concentration of the fibronectin clone following a 30 minute incubation period. The complex concentration is calculated assuming that the rate diffusion of the fibronectin clones to the EGFR at the surface is faster than the binding reaction (Da<<1), and thus, it can be assumed that the fibronectin concentration is constant. For this simulation, in the absence of measured values, all clones were assumed to have the same association rate (10^5 $M^{-1}s^{-1}$).

Associated Content

Supporting Information. Additional information as noted in the text. This material is available free of charge via the Internet at http://pubs.acs.org.

Acknowledgements

A NSF Graduate Research Fellowship to KK, Amgen Summer Scholar support to LC, a Burroughs Wellcome Fund Career Award at the Scientific Interface to HDS, the James H. Ferry Fund for Innovation and the Joseph R. Mares endowed chair supported this work. We thank Prof. K. Dane Wittrup for the gift of plasmids encoding the fibronectin clones his lab engineered to bind EGFR, for the crude protein mixtures containing EGFR that we further purified, and for a helpful conversation regarding typical on-rate variations that have been observed in past protein engineering efforts to improve binding affinity.

References

(1) Lou, X.; Lewis, M. S.; Gorman, C. B.; He, L. *Analytical Chemistry* **2005**, *77*, 4698–4705.

(2) Sikes, H. D.; Hansen, R. R.; Johnson, L. M.; Jenison, R.; Birks, J. W.; Rowlen, K. L.; Bowman, C. N. *Nature Materials* **2008**, *7*, 52–6.

(3) He, P.; Zheng, W.; Tucker, E. Z.; Gorman, C. B.; He, L. *Analytical chemistry* **2008**, *80*, 3633–9.

(4) Hansen, R. R.; Sikes, H. D.; Bowman, C. N. *Biomacromolecules* **2008**, *9*, 355–62.

(5) Hansen, R. R.; Avens, H. J.; Shenoy, R.; Bowman, C. N. *Analytical and Bioanalytical Chemistry* **2008**, *392*, 167–75.

(6) Avens, H. J.; Randle, T. J.; Bowman, C. N. *Polymer* **2008**, *49*, 4762–4768.

(7) Kuck, L. R.; Taylor, A. W. *BioTechniques* **2008**, *45*, 179–86.

(8) Hansen, R. R.; Johnson, L. M.; Bowman, C. N. *Analytical Biochemistry* **2009**, *386*, 285–7.

(9) Johnson, L. M.; Avens, H. J.; Hansen, R. R.; Sewell, H. L.; Bowman, C. N. *Australian journal of chemistry* **2009**, *62*, 877–884.

(10) He, P.; He, L. *Biomacromolecules* **2009**, *10*, 1804–9.

(11) Qian, H.; He, L. *Analytical Chemistry* **2009**, *81*, 4536–42.

(12) Qian, H.; He, L. *Analytical Chemistry* **2009**, *81*, 9824–7.

(13) Sikes, H. D.; Jenison, R.; Bowman, C. N. *Lab on a Chip* **2009**, *9*, 653–656.

(14) Avens, H. J.; Bowman, C. N. *Acta Biomaterialia* **2010**, *6*, 83–9.

(15) Avens, H. J.; Chang, E. L.; May, A. M.; Berron, B. J.; Seedorf, G. J.; Balasubramaniam, V.; Bowman, C. N. *Journal of Nanoparticle Research* **2010**, *13*, 331–346.

(16) Johnson, L. M.; Hansen, R. R.; Urban, M.; Kuchta, R. D.; Christopher, N. *Biomacromolecules* **2010**, *11*, 1133–1138.

(17) Avens, H. J.; Berron, B. J.; May, A. M.; Voigt, K. R.; Seedorf, G. J.; Balasubramaniam, V.; Bowman, C. N. *Journal of Histochemistry and Cytochemistry* **2011**, *59*, 76–87.

(18) Berron, B. J.; Johnson, L. M.; Ba, X.; McCall, J. D.; Alvey, N. J.; Anseth, K. S.; Bowman, C. N. *Biotechnology and bioengineering* **2011**, *108*, 1521–8.

(19) He, P.; Tucker, E. Z.; Gorman, C. B.; He, L. *Analytical Methods* **2011**, *3*, 2463.

(20) Lee, J. K.; Heimer, B. W.; Sikes, H. D. *Biomacromolecules* **2012**, *13*, 1136–1143.

(21) Berron, B. J.; May, A. M.; Zheng, Z.; Balasubramaniam, V.; Bowman, C. N. *Lab on a Chip* **2012**, *12*, 708–710.

(22) Kaastrup, K.; Sikes, H. D. *Lab on a chip* **2012**, *12*, 4055–4058.

(23) Wu, Y.; Liu, S.; He, L. *Analytical Chemistry* **2009**, *81*, 7015–7021.

(24) Wu, Y.; Liu, S.; He, L. *The Analyst* **2011**, *136*, 2558–63.

(25) Green, N. M. *Methods in Enzymology* **1970**, *18*, 418–424.

(26) Kuriyan, J.; Konforti, B.; Wemmer, D. In *The Molecules of Life*; Taylor & Francis Group, 2012.

(27) Sano, T.; Smith, C. L.; Cantor, C. R. *Science (New York, N.Y.)* **1992**, *258*, 120–2.

(28) Liang, M.; Klakamp, S. L.; Funelas, C.; Lu, H.; Lam, B.; Herl, C.; Umble, A.; Drake, A. W.; Pak, M.; Ageyeva, N.; Pasumarthi, R.; Roskos, L. K. *Assay and drug development technologies* **2007**, *5*, 655–62.

(29) Glass, T. R.; Ohmura, N.; Saiki, H. *Analytical chemistry* **2007**, *79*, 1954–60.

(30) Hackel, B. J.; Ackerman, M. E.; Howland, S. W.; Wittrup, K. D. *Journal of molecular biology* **2010**, *401*, 84–96.

(31) Afanassiev, V.; Hanemann, V.; Wölfl, S. *Nucleic acids research* **2000**, *28*, E66.

(32) Janin, J.; Chothia, C. *The Journal of biological chemistry* **1990**, *265*, 16027–16030.

(for TOC only)

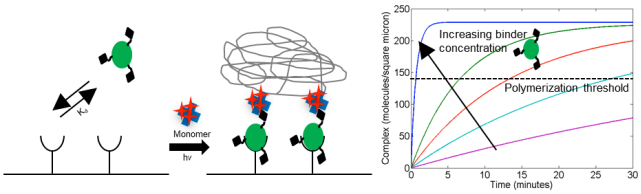
Monomer
hν
Increasing binder concentration
Polymerization threshold
Complex (molecules/square micron)
Time (minutes)
0
50
100
150
200
250
0
5
10
15
20
25
30

Supporting Information

The impact of dissociation constant on the detection sensitivity of polymerization-based signal amplification reactions

Kaja Kaastrup, Leslie Chan, and Hadley D. Sikes*

Department of Chemical Engineering, Massachusetts Institute of Technology, Cambridge, MA 02139

* To whom correspondence should be addressed
Tel: 617-324-4870
Fax: 617-253-2272
Email: sikes@mit.edu

Experimental Details

Materials

Poly(ethylene glycol) diacrylate (PEGDA) (M_n=575), triethanolamine (TEA), 1-vinyl-2-pyrrolidinone (VP), eosin Y disodium salt, sodium (meta) periodate, HABA, 10x phosphate buffered saline (PBS), 4'-hydroxyazobenzene-2-carboxylic acid (HABA), Triton® X-100, and Tween® 20 were purchased from Sigma Aldrich and used without further purification. Eosin 5-isothiocyanate was obtained from Marker Gene Technology. Streptavidin was purchased from Rockland Immunochemicals Inc. 10x bovine serum albumin blocker solution, EZ-Link NHS-LC biotin, and a BCA Protein Assay Kit with bovine serum albumin standards were purchased from Pierce/Thermo Scientific. 100x Denhardt's solution and Coomassie Brilliant Blue were obtained from Bioexpress. Glass slides (75x25x1 mm) were purchased from VWR. Seakem LE Agarose was purchased from Lonza. Imidazole (99%) was obtained from Alfa Aesar and cOmplete Mini Protease Inhibitor Cocktail was purchased from Roche. Rosetta™ host strains were purchased from Novagen. Sodium chloride, sodium phosphate monobasic, and sodium phosphate dibasic were purchased from Mallinckrodt Chemicals. Bacto agar and Difco LB broth were purchased from Becton, Dickinson, and Company. Chloramphenicol and kanamycin sulphate were obtained from Calbiochem. Isopropyl β-D-1 thiogalactopyranoside (IPTG) was purchased from Omega Bio-Tek. HisTrap™ FF crude 1 mL columns were purchased from GE Healthcare. Silicone isolators (9 mm diameter, 1 mm well depth) were obtained from Electron Microscopy Sciences. Cy3 NHS ester was purchased from Lumiprobe. UltraCruz™ Micro G-25 Spin Columns were purchased from Santa Cruz Biotechnology, Inc. 4-15% Mini-PROTEAN® TGX™ Precast Gels were purchased from Bio-Rad Laboratories, Inc.

Protein Expression and Biotinylation

Plasmids (pEThK-Fn3 clones B, D, and E)[30] were obtained from the K.D. Wittrup Lab. To express each clone, plasmids were transformed into Rosetta (DE3) E. coli, which were then grown on LB agar plates (with 30 mg/mL kanamycin and 25 mg/mL chloramphenicol) at 37°C. Starter cultures were prepared by transferring single colonies to 5 mL of LB media (with 30 mg/L kanamycin and 25 mg/mL chloramphenicol). These cultures were grown at 37°C at 250 rpm for ~16 hours and then added to 100 mL of LB media (with 30 mg/L kanamycin and 25 mg/mL chloramphenicol) in a 250 mL flask to be grown at 37°C and 250 rpm. Once the absorbance at 600 nm had reached ~1, expression was induced by adding IPTG to a final concentration of 0.5 mM. The cells were then incubated for a further 24 hours at 37°C and 250 rpm. At this point, the cells were pelleted at 15,000xg for 15 minutes (4°C). The supernatant was decanted and the cells were resuspended in 25 mL wash buffer (300 mM NaCl, 50 mM sodium phosphate, 10 mM imidazole, pH 7.4). A cOmplete Mini protease inhibitor cocktail tablet was added to the cell suspension. The sample tube containing the cell mixture was placed in a container packed with ice and sonicated 3 times for 60 seconds each (Branson sonifier 250, output control set to 5, 50% duty cycle). The sample was centrifuged at 15,000xg for 15 minutes (4°C) and the supernatant was filter sterilized with a 0.2 μm filter in preparation for metal affinity purification. The proteins were purified using an ÄKTAFPLC and HisTrap FF Crude columns. The elution buffer consisted of 300 mM NaCl, 50 mM sodium phosphate, 300 mM imidazole (pH 7.6). (Supplementary Figure 1)

Following purification, the proteins were biotinylated with the EZ-Link NHS-LC-Biotin and subsequently purified using UltraCruz™ Micro G-25 Spin Columns. Total protein was quantified using a BCA assay with BSA standards.

HABA Assay for determining relative degree of biotinylation

A standard curve for determining the degree of biotinylation was generated by adding varying concentrations of biotin to HABA-streptavidin solutions. The standards were prepared in a 96-well microplate format; 20 µL of various concentrations of biotin stock solutions in pH 6, 0.05 M sodium phosphate, 0.15 M NaCl buffer were added to 180 µL HABA-streptavidin (175.6 µL 0.5 mg/mL streptavidin in pH 6, 0.05 M sodium phosphate, 0.15 M NaCl buffer and 4.4 µL 2.42 mg/mL HABA in 10 mM NaOH). The samples were prepared by mixing 20 µL of each biotinylated protein with 180 µL of the HABA-streptavidin solution. The samples were mixed for 5 minutes prior to reading the absorbance at 500 nm using a Plate Reader. The standard curve was constructed by plotting the change in absorbance for the biotin dilutions (relative to a sample to which 20 µL of buffer had been added) as a function of biotin concentration.
(Supplementary Figure 2)

Densitometry

Because the BCA assay determines the total amount of protein, the fraction of the total corresponding to each of the fibronectin clones was estimated using densitometry. Duplicate samples of each of the fibronectin clone protein purifications were run at a total protein concentration of 1.5 µg on an SDS-PAGE gel along with BSA standards (2 µg, 1.5 µg, and 1 µg). Following Coomassie staining, the gel was imaged and analyzed using ImageJ. The image was

inverted and the integrated intensities of equal areas fully encompassing each of the protein bands as well as an area removed from the bands (to be used as the background intensity) were measured. The integrated intensities were then background corrected and the quantity of each of the fibronectin clones was determined through normalization by the integrated intensity of the BSA standard bands. (Supplementary Figure 3)

EGFR/Fc purification

An EGFR (extracellular domain)-Fc receptor fusion was isolated from a mixture of EGFR-Fc fusion and Fc receptor using size exclusion chromatography (Superdex 75 10/300 GL gel filtration column). The resulting fractions were collected and run on an SDS-PAGE gel to identify the fraction containing the fusion. Fraction 7 contained the fusion without any contaminating Fc. (Supplementary Figure 4)

Details of Aldehyde Functionalized Agarose Surface Preparation

2 mL of a solution of 0.2 wt% agarose in distilled water (briefly heated in the microwave) were pipetted onto a glass slide and dehydrated overnight under ambient conditions. Activation of the agarose was achieved by immersing the slides in 20 mM sodium (meta) periodate (in distilled water) for 30 minutes. Following activation, the surfaces were rinsed with distilled water and dried under ambient conditions for 2 hours prior to protein printing.

Antigen Density Determination

We quantified the number of binding-accessible EGFR molecules per square micron in each spot using a streptavidin-Cy3 conjugate and fluorescence analysis (Agilent microarray scanner)

against a Cy3 calibration array (Full Moon Biosystems). The surfaces were developed according to the standard protocol; in brief, the surfaces were blocked for 10 minutes with 1% BSA in 1x PBS and rinsed with 1x PBS, 40 μL of each of the biotinylated fibronectin clones (10 μg/mL total protein) was added to separate isolators and the binding interaction was given 30 minutes to reach completion before unbound protein was rinsed away using 1x PBS. At this point, the test surfaces were contacted with 0.1 μM streptavidin-Cy3 in 0.75% BSA in 1.5x PBS, 5x Denhardts for five minutes in a humid chamber. Sequential rinses with PBST (1x PBS, 0.1% Tween 20), 1x PBS, and ddH_2O were used to remove unbound streptavidin-Cy3. The background fluorescence was determined by preparing surfaces with the corresponding unbiotinylated fibronectin clones in place of the biotinylated binders. The fluorescence intensity of the EGFR spots was then quantified and subtracted from the fluorescence intensity of features contacted with the biotinylated binders. These background-corrected fluorescence signals were compared with a standard curve generated using the Full Moon Biosystems calibration array where features containing only spotting buffer were used to calculate background signal. The arrays were scanned at 100% PMT with an excitation wavelength of 532 nm (20 mW) and emission wavelengths between 550 and 610 nm.

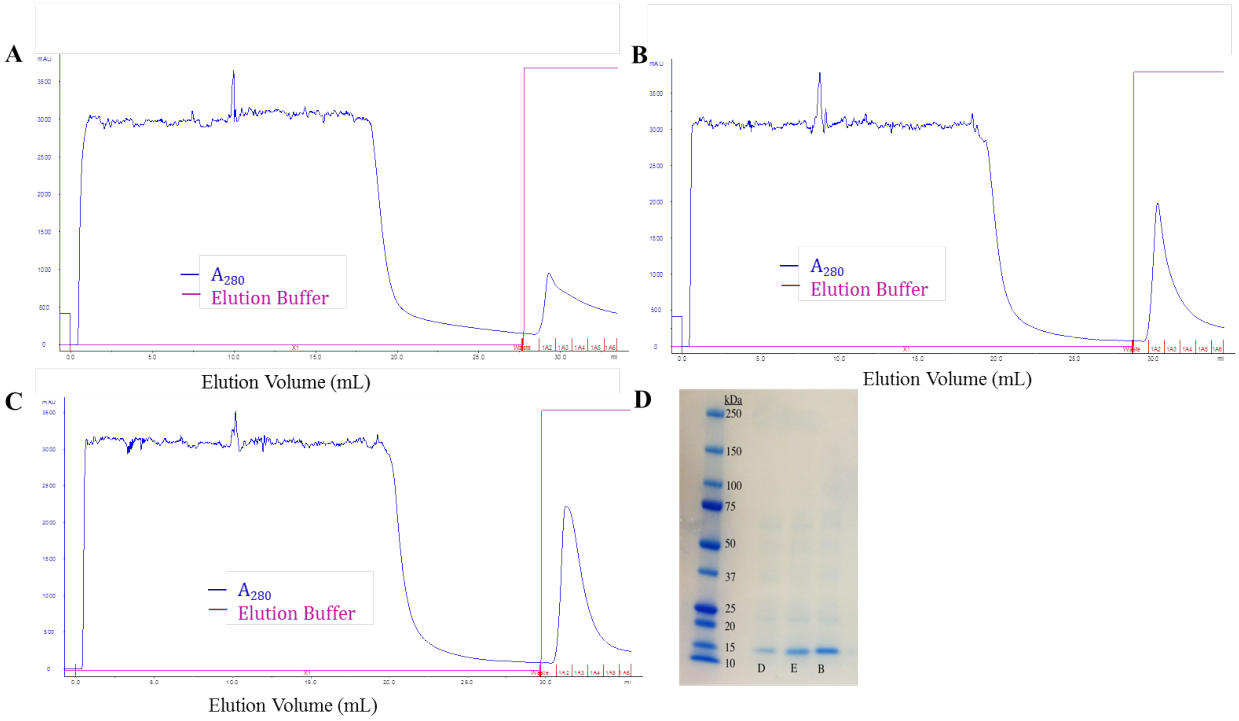

Supplementary Figure 1. Fibronectin clone purifications. (A) Chromatogram for metal affinity purification of clone B showing the absorbance at 280 nm and the introduction of elution buffer. The fractions eluted (in red) were pooled and the amount of protein was quantified using a BCA assay. (B) Chromatogram for metal affinity purification of clone D showing the absorbance at 280 nm and the introduction of elution buffer. The fractions eluted (in red) were pooled and the amount of protein was quantified using a BCA assay. (C) Chromatogram for metal affinity purification of clone E showing the absorbance at 280 nm and the introduction of elution buffer. The fractions eluted (in red) were pooled and the amount of protein was quantified using a BCA assay. (D) SDS-PAGE gel. Based on total protein quantification (BCA assay), 1.5 µg of each of the protein purifications was loaded onto an SDS-PAGE gel, which was then run for 30 minutes at 150 V.

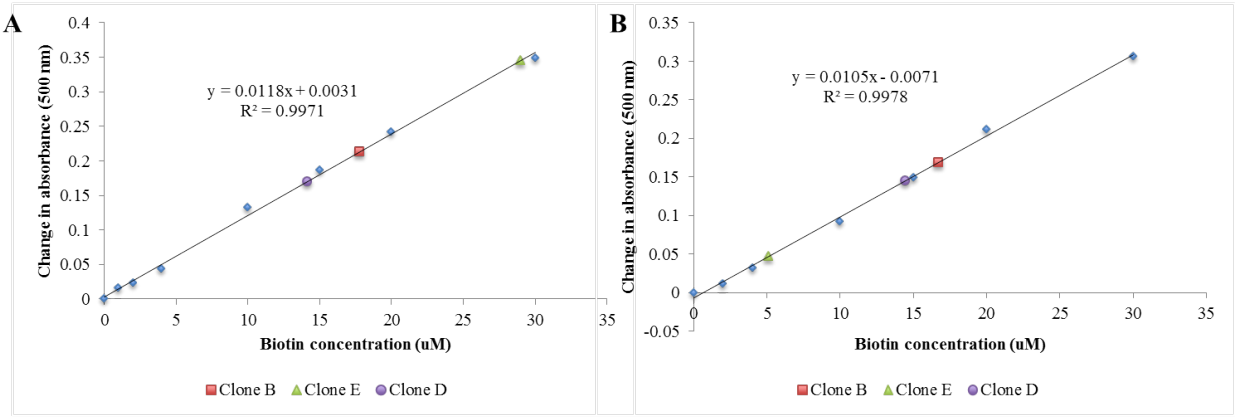

C

Fibronectin clone	Biotin/protein (standard curve A)	Biotin/protein (standard curve B)
D	10	10
E	8	7
B	12	11

Supplementary Figure 2. HABA assay on biotinylated fibronectin clones. (A) Standard curve for determining the degree of biotinylation generated by adding varying concentrations of biotin to HABA-streptavidin solutions. The change in absorbance for the biotin dilutions (relative to a sample to which no biotin was added) is plotted as a function of biotin concentration. The change in absorbance for each of the clones is shown on the plot. (B) Replicate HABA assay performed on a different day. (C) Table summarizing the number of biotin per protein determined using the two separate standard curves. The number of biotin per protein is defined as the moles of biotin (as indicated by the assay) divided by the moles of protein (based on a BCA assay and assuming that there are not any contaminating proteins present). Because the proteins differ only with respect to a small subset of amino acids, it is reasonable to assume that they are similarly reactive; therefore, we hypothesize that the differences in the number of biotin per protein are attributable to differences in the relative purities of the protein preparations.

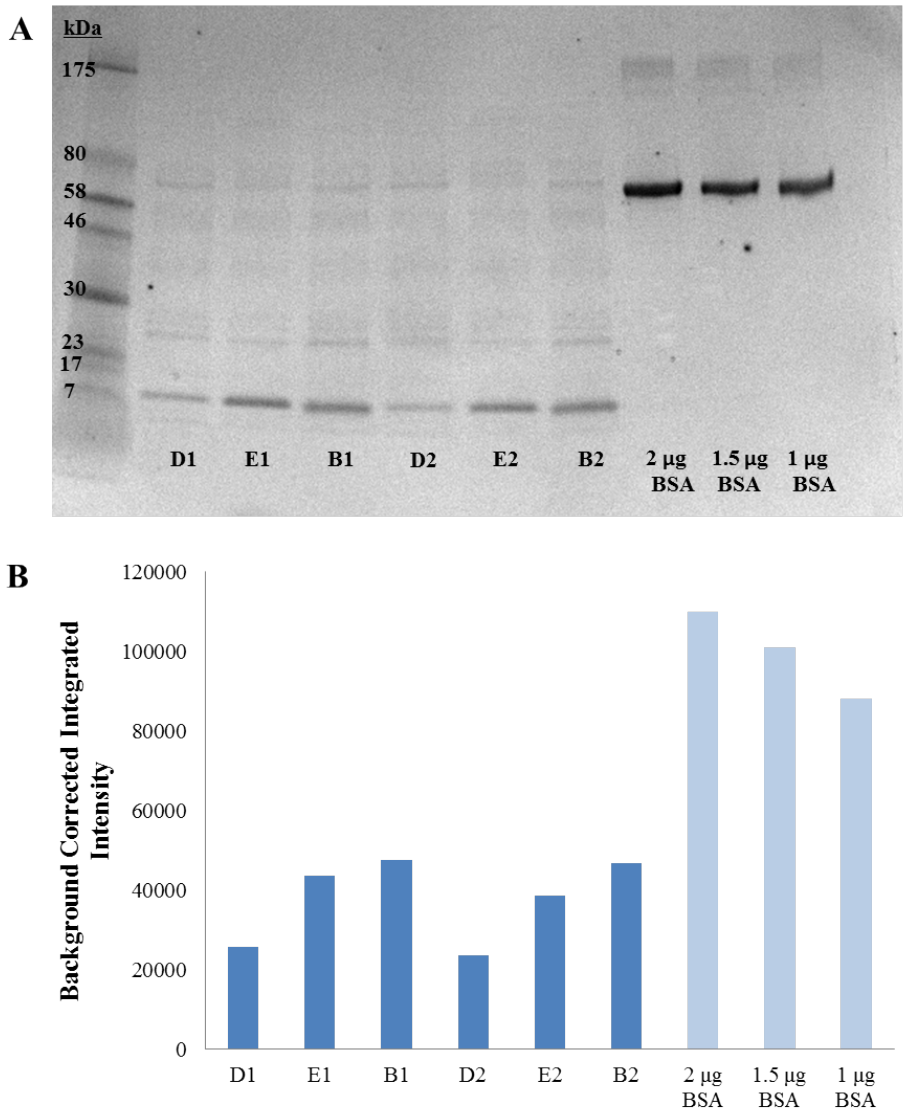

Supplementary Figure 3. Densitometric analysis. (A) SDS-PAGE gel. 1.5 µg total protein (based on a BCA assay) of each fibronectin clone protein preparation was loaded in duplicate onto an SDS-PAGE gel along with a protein ladder and BSA standards at the indicated quantities. The gel was imaged and densitometric analysis was performed in order to determine the amount of each fibronectin clone in the respective protein preparations. (B) Quantification of the SDS-PAGE gel presented in A. Using ImageJ, the image was inverted and the integrated intensities of equal areas fully encompassing the bands as well as an area removed from the bands (to be used as the background intensity) were measured. The integrated intensities were then background corrected (shown above) and the quantity of each of the fibronectin clones was determined through normalization by the integrated intensity of the BSA standard bands.

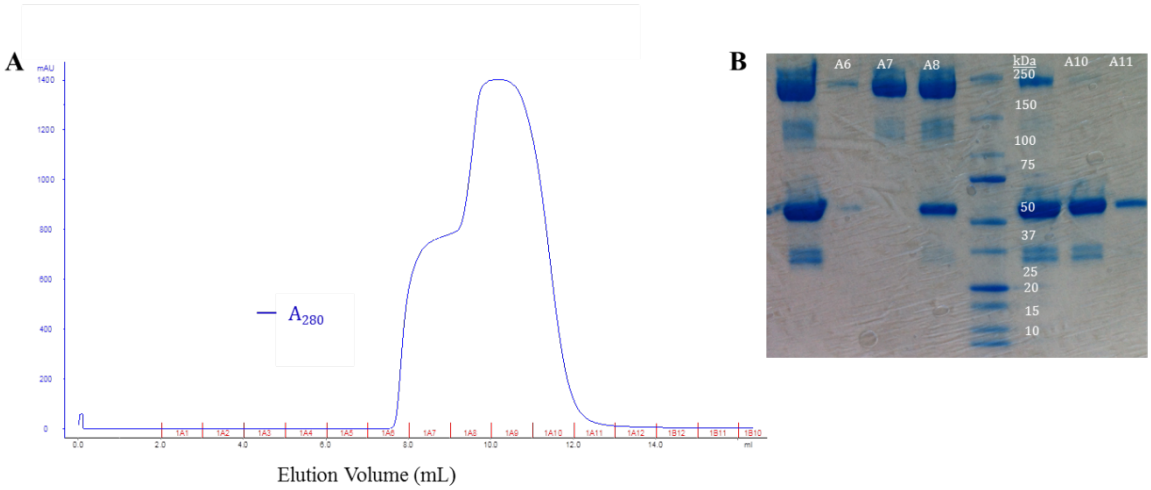

Supplementary Figure 4. EGFR-Fc fusion purification. (A) Chromatogram for size exclusion purification of the EGFR-Fc fusion showing the absorbance at 280 nm. (B) SDS-PAGE gel of fractions collected during the size exclusion purification. The fractions collected from the size exclusion purification of the EGFR-Fc fusion were diluted 1:1 with Laemmli buffer and loaded onto an SDS-PAGE gel (run at 150 V for 30 minutes). The fraction collected of the EGFR-FC fusion and used in this study is labeled A7.

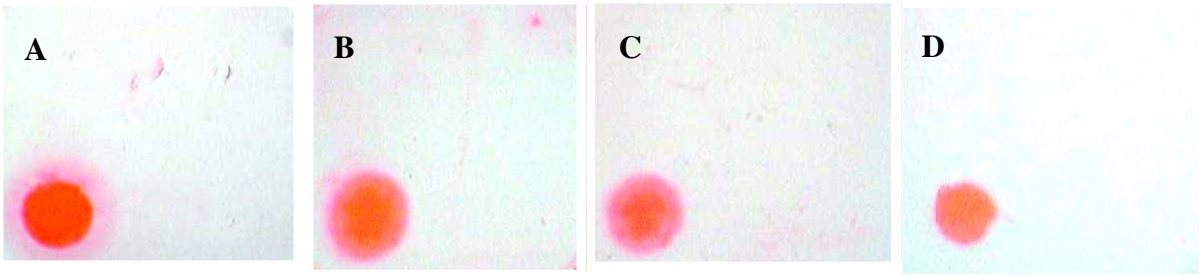

Supplementary Figure 5. Negative and positive controls. (A) The test surface was prepared omitting the incubation with a biotinylated fibronectin clone. This demonstrates that nonspecific binding of streptavidin-eosin to EGFR does not result in a false positive. (B) The test surface was prepared with 1 uM unbiotinylated clone B in place of its biotinylated counterpart. (C) The test surface was prepared with 1 uM unbiotinylated clone E in place of its biotinylated counterpart. (D) The test surface was prepared with 1 uM unbiotinylated clone D in place of its biotinylated counterpart. The latter three cases demonstrate that nonspecific binding of streptavidin-eosin to the fibronectin clones does not result in a false positive. In all cases, polymerization is observed in response to the binding of the streptavidin-eosin conjugate to the biotin covalently coupled to the surface as the positive control spot.

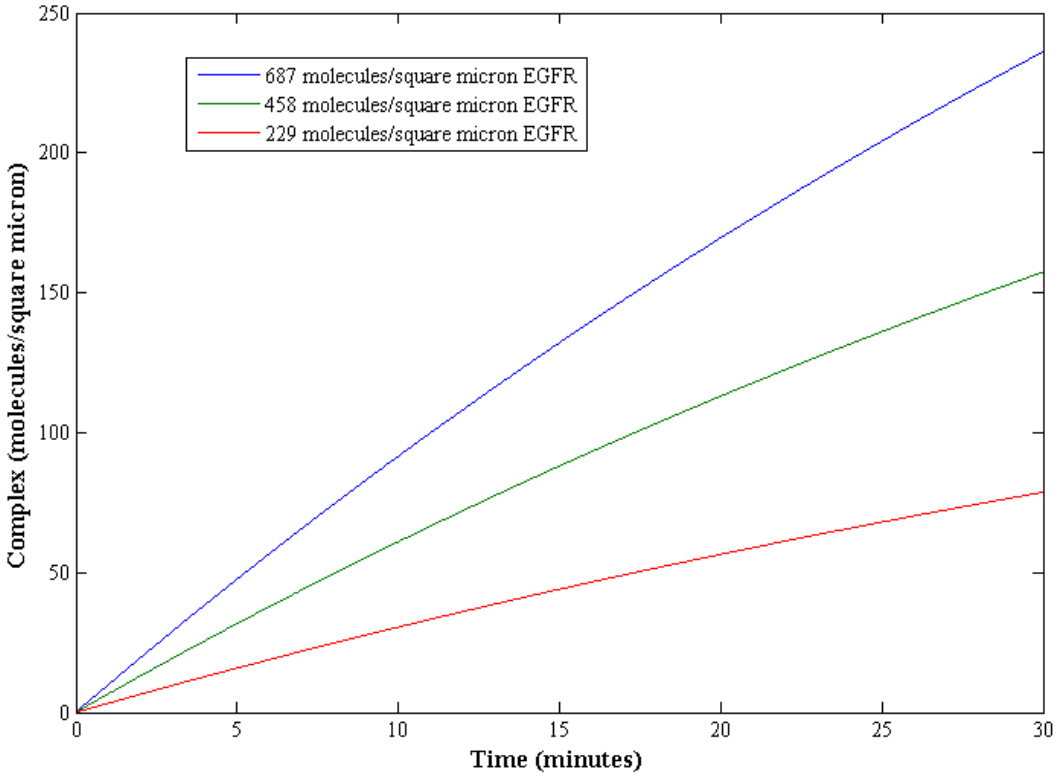

Supplementary Figure 6. Complex concentration increases as the concentration of immobilized EGFR molecules increases. Complex concentration as a function of time is shown for the EGFR surface density determined experimentally (229 molecules/μm^2) as well as double and triple this concentration. For the results generated above, the concentration of fibronectin clone D (K_d=0.25 nM) was set to 2.4 nM. The experimental data (Figure 3 in the text) shows that the initiator density achieved with a surface density of 229 molecules EGFR/μm^2 and 2.4 nM of clone D in solution is not sufficient after a 30-minute incubation to initiate polymerization. This simulation shows that one way to achieve an initiator density above the threshold required for polymerization while holding the solution concentration of the target biomolecule (clone D) constant would be to increase the surface density of EGFR.

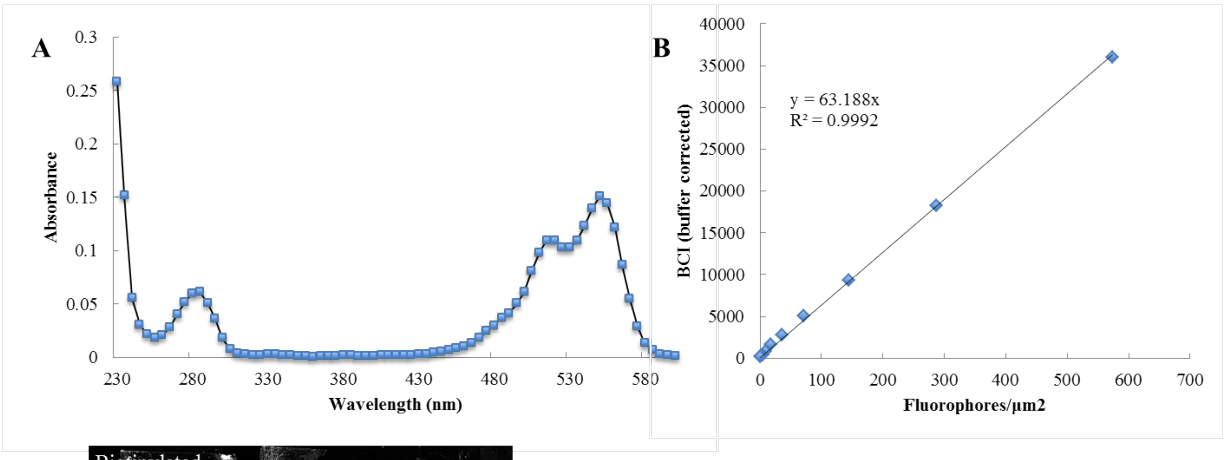

D **Streptavidin per square micron**

Fibronectin Clone	EGFR (1)	EGFR (2)	Positive Control	Negative Control
10 µg/mL B-b	220	230	270	60
10 µg/mL E-b	260	260	270	30
10 µg/mL D-b	230	180	240	70
Average	230		260	50

Supplementary Figure 7. Protein surface density quantification. (A) A streptavidin-Cy3 conjugate with 3.5 Cy3 molecules per streptavidin was prepared using the same method outlined above, though with a NHS ester-functional dye in the place of an isothiocyanate dye. Extinction coefficients used in the analysis: $\varepsilon_{cy3,552} = 150{,}000\ M^{-1}cm^{-1}$, $\varepsilon_{cy3,280} = 12{,}000\ M^{-1}cm^{-1}$ $\varepsilon_{SA,280} = 173{,}000\ M^{-1}cm^{-1}$. (B) Standard curve generated using a Full Moon Biosystems calibration array. The signal intensities were determined using ImageJ to compute average intensities within specified regions of constant area. BCI (background corrected intensity) is defined as the difference between the signal and the background (in the case of the calibration array, an array of buffer spots). The array was scanned at 100% PMT with an excitation wavelength of 532 nm (20 mW) and emission wavelengths between 550 and 610 nm. (C) (Top) A biochip test surface reacted with 10 µg/mL (total protein) of each of the biotinylated fibronectin clones (from left to right: clones B, E, and D) followed by 0.1 µM streptavidin-Cy3 conjugate as described in the text and imaged using an Agilent microarray scanner with an excitation wavelength of 532 nm (20 mW) and emission wavelengths between 550 nm and 610 nm. The PMT setting was 100%. The top two features in each array correspond to the EGFR-Fc fusion immobilized on the surface, while the bottom right feature is the positive control spot (biotinylated clone B). The rightmost array demonstrates how surface defects (arising through contact with the end of a pipet tip, for example) can result in false positives. (Bottom) A biochip test surface developed in the same way as the top image with the exception that the surface has been reacted with 10 µg/mL (total protein) of each of the unbiotinylated fibronectin clones (from left to right: clones B, E, and D). (D) Table summarizing the number of streptavidin bound per square micron for the indicated surface features based on average signal intensities determined using the images presented in (C). The bottom image in (C) was used as the background correction for the top image and the intensity values were converted to the number of streptavidin bound per square micron using the calibration array standard curve (B).

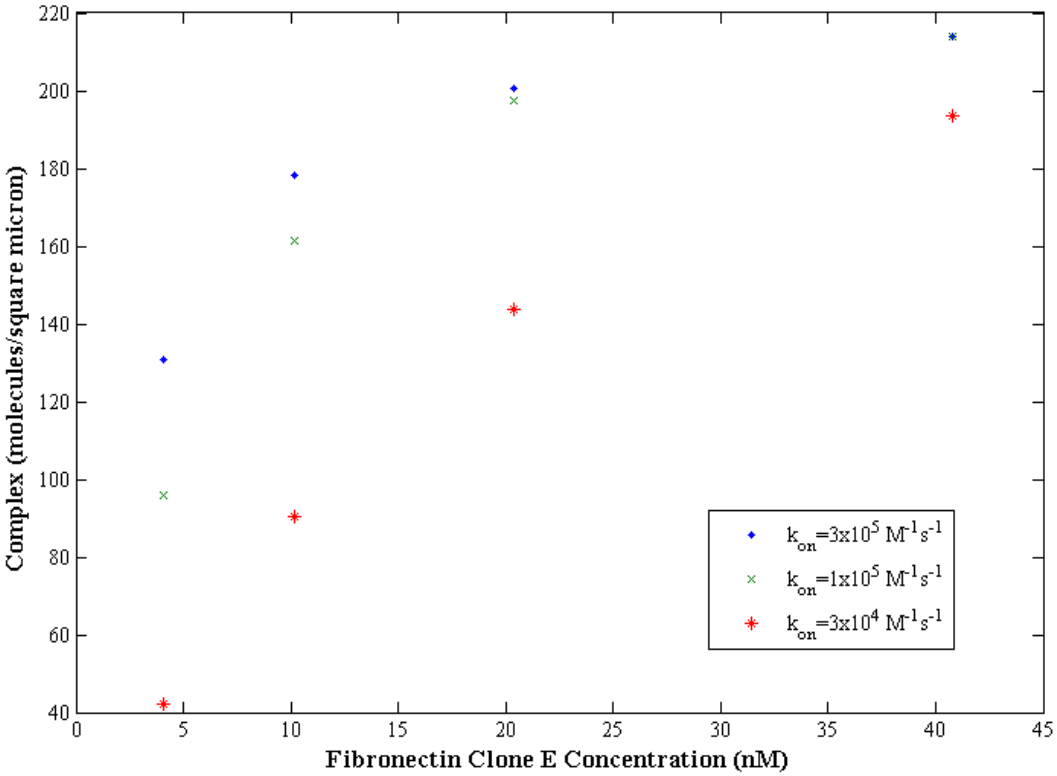

Supplementary Figure 8. Reducing the on-rate below 10^5 $M^{-1}s^{-1}$ results in a reduction in the complex concentration for lower concentrations of the fibronectin clone. For the results generated above, K_d=2.9 nM (fibronectin clone E) and the binding reaction time was set to 30 minutes. This simulation shows the extent to which slight changes in the on-rate (which may occur from clone to clone as clones were selected using equilibrium titrations rather than kinetic screens) result in changes in the surface concentration of the EGFR-Fn complex. For example, looking at the 10 nM points, a deviation of the on-rate from the standard order-of-magnitude assumption of 10^5 $M^{-1}s^{-1}$ could place the initiator density either well above or well below the observed threshold required for polymerization.

A

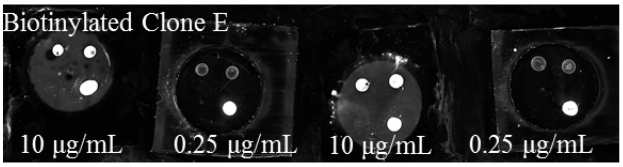

B

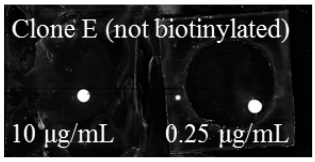

C **Streptavidin per square micron**

Fibronectin Clone	EGFR (average of 4)
10 µg/mL E-b	240
0.25 µg/mL E-b	70

Supplementary Figure 9. Protein surface density quantification for clone E. (A) A biochip test surface reacted with the indicated concentration (total protein) of biotinylated fibronectin clone E followed by 0.1 µM streptavidin-Cy3 conjugate as described in the text and imaged using an Agilent microarray scanner with an excitation wavelength of 532 nm (20 mW) and emission wavelengths between 550 nm and 610 nm. The PMT setting was 100%. The top two features in each array correspond to the EGFR-Fc fusion immobilized on the surface, while the bottom right feature is the positive control spot (biotinylated clone B). Based on densitometry, 10 µg/mL clone E corresponds to 410 nM and 0.25 µg/mL corresponds to 10 nM. (B) A biochip test surface developed as described for A, with the exception that unbiotinylated clone E was used in place of the biotinylated clone. (C) Table summarizing the number of streptavidin bound per square micron for the EGFR surface features based on average signal intensities determined using the images presented in A and B. The fluorescence intensities of the relevant features in the image in B were used as the background correction for the image in A and the intensity values were converted to the number of streptavidin bound per square micron using the calibration array standard curve shown in Supplementary Figure 7B.